Atropisomerization of *cis*-Bis(5'GMP)-Platinum(II)-Diamine Complexes with Non-C_2-Symmetrical Asymmetric Diamine Ligands Containing NH Groups Directed to One Side of the Coordination Plane

Danita Kiser,† Francesco P. Intini,‡ Yinghai Xu,† Giovanni Natile,*,‡ and Luigi G. Marzilli*,†

Department of Chemistry, Emory University, Atlanta, Georgia 30322, and Dipartimento Farmaco-Chimico, Facoltà di Farmacia, Università degli Studi di Bari, 70125 Bari, Italy

Received March 9, 1994®

Complexes of the type LPt(5'GMP)$_2$, where L = *N*,*N*'-dimethyl-2,3-diaminobutane and the stereochemistries at the four asymmetric centers (N, C, C, N) are *S*,*R*,*R*,*R* and *S*,*S*,*S*,*R*, were prepared at pH 3.5 from the respective LPt(SO$_4$) compounds by treating with 2 equiv of 5'GMP. These complexes have both diamine NH groups directed to the same side of the coordination plane. The resulting 5'GMP complexes were studied by using 1D and 2D NMR methods. NOE data demonstrate that the 5'GMPs are coordinated via N7 to two nonequivalent Pt coordination sites. Restricted rotation about the Pt–N7 bonds potentially could lead to four different atropisomers for each complex: two head-to-tail (HT) and two head-to-head (HH) species with the H8s of the 5'GMP on the opposite side and on the same side of the Pt coordination plane, respectively. Four atropisomers would exhibit a total of eight H8 signals. However, for both species, four major H8 signals were observed in two sets of two signals. Thus, two major atropisomers were present for each LPt(5'GMP)$_2$ complex. For each complex, cross-peaks observed in the H8 region of the NOESY/EXSY and ROESY spectra indicated exchange by rotation about the Pt–N7 bond. From assignments of the *N*,*N*'-dimethyl-2,3-diaminobutane proton signals via COSY spectra and subsequent comparisons of the intensities of H8–NH to H8–NCH$_3$ cross-peaks, the conformations and chirality of the major atropisomers were systematically determined. The chelate ring of the diamine is puckered and has the λ conformation in (*S*,*R*,*R*,*R*)-LPt(5'GMP)$_2$ and the δ conformation in (*S*,*S*,*S*,*R*)-LPt(5'GMP)$_2$. For both the (*S*,*R*,*R*,*R*)-LPt(5'GMP)$_2$ and the (*S*,*S*,*S*,*R*)-LPt(5'GMP)$_2$ complexes, the two major atropisomers have the HT conformation. For the (*S*,*R*,*R*,*R*)-LPt(5'GMP)$_2$ complex, two HH atropisomers were also identified on the basis of the chemical shifts of their 5'GMP H8 signals and the unique pattern of cross peaks in the H8 region. However, the HT conformation is preferred 10:1 (HT:HH). For the (*S*,*S*,*S*,*R*)-LPt(5'GMP)$_2$ complex, the relative amount of the HH species is probably very small since no signals for the two HH atropisomers were clearly observed. Several factors, including O6–NH and ROPO$_3$–NH hydrogen bonding, play a role in determining conformation and abundance of the atropisomers.

Introduction

Anticancer compounds such as *cis*-Pt(NH$_3$)$_2$Cl$_2$ and Pt(en)Cl$_2$ preferentially attack purine moieties in DNA,[1] the most common point of attack being the N7 of guanine.[2-4] The nature of the nonleaving groups, i.e. the amine ligands, plays an important, but not completely defined role in the anticancer activity of the drug. The requirement that at least one hydrogen be attached to each amine for significant anticancer activity[5-7] has led to the speculation that this NH group forms a hydrogen bond to the O6 of guanine[8,9] or a phosphate oxygen.[10-18] In DNA, these platinum compounds cross-link adjacent purine residues[2-4] in a head-to-head (HH) conformation in which both the H8 atoms are on the same side of the platinum coordination plane.[12,13,17,19-24] When the two nucleot(s)ide moieties are not linked by a phosphodiester group, the purines can have orientations in which the H8s are on opposite sides of the platinum coordination plane; this orientation is designated head-to-tail (HT). Normally only HT complexes are detected in solution and in most solid-state crystallographic studies.[25-27] The HH atropisomers are difficult to isolate and have been found in only a few crystal structures of *cis*-[Pt(NH$_3$)$_2$-

† Emory University.
‡ Università degli Studi di Bari.
• Abstract published in *Advance ACS Abstracts*, July 15, 1994.

(1) Mansy, S.; Chu, G. Y. H.; Duncan, R. E.; Tobias, R. S. *J. Am. Chem. Soc.* **1978**, *100*, 607.
(2) Fichtinger-Schepman, A. M. J.; van der Veer, J. L.; den Hartog, J. H. J.; Lohman, P. H. M.; Reedijk, J. *Biochemistry* **1985**, *24*, 707.
(3) Fichtinger-Schepman, A. M. J.; van Oosterom, A. T.; Lohman, P. H. M.; Berends, F. *Cancer Res.* **1987**, *47*, 3000.
(4) Eastman, A. *Biochemistry* **1986**, *25*, 3912.
(5) Reedijk, J.; Fichtinger-Schepman, A. M. J.; van Oosterom, A. T.; van de Putte, P. *Struct. Bonding (Berlin)* **1987**, *67*, 53.
(6) Johnson, N. P.; Butour, J.-L.; Villani, G.; Wimmer, F. L.; Defais, M.; Pierson, V.; Brabec, V. *Prog. Clin. Biochem. Med.* **1989**, *10*, 1.
(7) Sundquist, W. I.; Lippard, S. J. *Coord. Chem. Rev.* **1990**, *100*, 293.
(8) Xu, Y.; Natile, G.; Intini, F. P.; Marzilli, L. G. *J. Am. Chem. Soc.* **1990**, *112*, 8177.
(9) Hambley, T. W. *Inorg. Chem.* **1988**, *27*, 1073.
(10) den Hartog, J. H. J.; Altona, C.; van der Marel, G. A.; Reedijk, J. *Eur. J. Biochem.* **1985**, *147*, 371.
(11) Bloemink, M. J.; Heetebrij, R. J.; Inagaki, K.; Kidani, Y.; Reedijk, J. *Inorg. Chem.* **1992**, *31*, 4656.
(12) Fouts, C. S.; Marzilli, L. G.; Byrd, R. A.; Summers, M. F.; Zon, G.; Shinozuka, K. *Inorg. Chem.* **1988**, *27*, 366.
(13) Berners-Price, S. J.; Frenkiel, T. A.; Ranford, J. D.; Sadler, P. J. *J. Chem. Soc., Dalton Trans.* **1992**, 2137.
(14) Berners-Price, S. J.; Frey, U.; Ranford, J. D.; Sadler, P. J. *J. Am. Chem. Soc.* **1993**, *115*, 8649.
(15) Kozelka, J.; Petsko, G. A.; Lippard, S. J.; Quigley, G. J. *J. Am. Chem. Soc.* **1985**, *107*, 4079.
(16) Sherman, S. E.; Gibson, D.; Wang, A. H.-J.; Lippard, S. J. *Science* **1985**, *230*, 412.
(17) Sherman, S. E.; Gibson, D.; Wang, A. H.-J.; Lippard, S. J. *J. Am. Chem. Soc.* **1988**, *110*, 7368.
(18) Reedijk, J. *Inorg. Chim. Acta* **1992**, *198–200*, 873.
(19) Mukundan, S., Jr.; Xu, Y.; Zon, G.; Marzilli, L. G. *J. Am. Chem. Soc.* **1991**, *113*, 3021.
(20) Caradonna, J. P.; Lippard, S. J. *Inorg. Chem.* **1988**, *27*, 1454.
(21) Neumann, J.-M.; Tran-Dinh, S.; Girault, J.-P.; Chottard, J.-C.; Huynh-Dinh, T.; Igolen, J. *Eur. J. Biochem.* **1984**, *141*, 465.
(22) Kline, T. P.; Marzilli, L. G.; Live, D.; Zon, G. *J. Am. Chem. Soc.* **1989**, *111*, 7057 and references cited therein.
(23) den Hartog, J. H. J.; Altona, C.; van Boom, J. H.; van der Marel, G. A.; Haasnoot, C. A. G.; Reedijk, J. *J. Biomol. Struct. Dyn.* **1985**, *2*, 1137.
(24) Admiraal, G.; van der Veer, J. L.; de Graff, R. A.; den Hartog, J. H. J.; Reedijk, J. *J. Am. Chem. Soc.* **1987**, *109*, 592.

0020-1669/94/1333-4149$04.50/0

$(9\text{-EtGH})_2]X_2$.[28,29] Recently, HH species have been found in octahedral complexes of 1,5,6-trimethylbenzimidazole with Ru(II) and Re(V).[30]

It has been proposed that, in solution, rotation about the Pt–N7 bond is crucial in forming the DNA lesion between adjacent purines.[26,31-37] In bis complexes *cis*-PtA_2(nucleot(s)ide-N7)$_2$ (A_2 is two unidentate or one bidentate amine ligand and N7 indicates binding through N7 of a purine nucleot(s)ide), rotation about the Pt–N7 bond leads to interconversion between atropisomers. For 6-oxopurine nucleot(s)ides, a nonbulky A_2 allows fast rotation on the NMR time scale;[31,32,38] this rotation is demonstrated by the observation of only one H8 signal. When A_2 is bulky, restricted rotation becomes evident by the appearance of more than one H8 signal.[8,26,31-38] Restricted rotation has been demonstrated even when A_2 is not bulky. In some *cis*-PtA_2(nucleot(s)ide)$_2$ adducts with N7 of adenine or N3 of cytosine bound to platinum, the rate of rotation is slowed enough such that several different *cis*-PtA_2(nucleot(s)ide)$_2$ atropisomers are detected via NMR studies.[26,39] This situation arises from the greater bulk flanking the binding site of these ligands compared to the N7 site of 6-oxopurine derivatives.[26,39]

The asymmetry of the ribose moiety influences the number of signals that can be observed in the NMR spectrum. In bis 6-oxopurine nucleot(s)ide *cis*-PtA_2 complexes with bulky, C_2 symmetrical A_2 ligands, the two HT atropisomers are distinguishable by NMR due to the asymmetry of the sugar.[31] When viewing the *cis*-PtA_2(nucleot(s)ide)$_2$ complex from the nucleot(s)ide coordination side, the conformation in which an imaginary line drawn through an equivalent point in both purines, H8, has a negative slope is defined as ΔHT.[32] For the ΛHT conformation, this line has a positive slope.[32] Each HT atropisomer has one H8 signal. Only one HH atropisomer is possible in such *cis*-PtA_2(nucleot(s)ide)$_2$ complexes, but the H8s are nonequivalent so two signals are expected; this leads to four possible H8 signals for such cis, bis complexes. If the *cis*-PtA_2 moiety lacks local C_2 symmetry (e.g., two different A (A, A′) or an unsymmetrical chelate) each H8 is nonequivalent for both HT atropisomers,[26,35,36] leading to four total H8 signals for the HT atropisomers. Two HH species are now possible in which each H8 is again nonequivalent; therefore, four signals could be observed. Thus a total of eight H8 signals are possible for such cis bis products.

The particular *cis*-PtA_2 or *cis*-PtAA′ moiety designed for our studies is LPt, where L = *N*,*N*′-dimethyl-2,3-diaminobutane. The stereochemistry of the carbon methyl groups on the backbone influences the stereochemistry at nitrogen, limits ligand flexibility, and increases bulk. (For simplicity, the *N*,*N*′-dimethyl-2,3-diaminobutane ligands will be abbreviated according to their stereochemistry). A recent investigation of complexes of the type

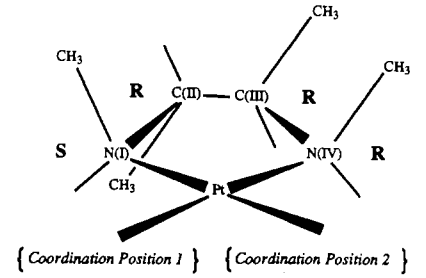

[(S,R,R,R)-N,N'-dimethyl-2,3-diaminobutane]Pt(II)

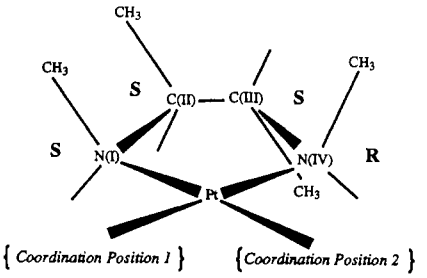

[(S,S,S,R)-N,N'-dimethyl-2,3-diaminobutane]Pt(II)

Figure 1. Stick representation of the two *N*,*N*′-dimethyl-2,3-diaminobutane platinum moieties. Roman numerals label the chelate ring nitrogens and carbons. The 5′GMP coordination positions are labeled according to the text.

(*R*,*S*,*S*,*R*)-LPt(5′GMP)$_2$ (where the configurations at the four asymmetric centers are *R*, *S*, *S*, and *R* at N, C, C, and N, respectively) led to the first evidence for the existence of a HH atropisomer in solution.[8] In addition, the HH atropisomer was found to exist in equilibrium with two HT atropisomers, the predominant HT having the ΛHT conformation. This was the first determination of the chirality of a HT species in solution; the ΔHT conformation had been found in all documented solid state structures for 6-oxopurine nucleot(s)ide complexes with metal centers.[25,37,40] For the complex with all asymmetric centers on L inverted, (*S*,*R*,*R*,*S*)-LPt(5′GMP)$_2$, the dominant atropisomer had the ΔHT conformation. This result demonstrated that the stereochemistry of the amine ligand influences the conformational equilibrium between atropisomers. The use of platinum(II) complexes of stereochemically controlling bulky ligands such as *N*,*N*′-dimethyl-2,3-diaminobutane showed promise for controlling DNA or RNA conformations.

In this study, we investigated LPt(5′GMP)$_2$ complexes with L configurations *S*,*R*,*R*,*R* and *S*,*S*,*S*,*R*. The two nonequivalent platinum coordination positions of the (*S*,*S*,*S*,*R*)- and (*S*,*R*,*R*,*R*)-LPt moieties (Figure 1) are designated as coordination positions 1 and 2, ***cp1*** and ***cp2***, respectively. The structures are presented with the square plane of the platinum complex perpendicular to the plane of the paper and with the L backbone to the rear. The nitrogen and carbon atoms along the L backbone are distinct and are labeled I, II, III, and IV.

The (*S*,*R*,*R*,*R*)-LPt and the (*S*,*S*,*S*,*R*)-LPt moieties are enantiomeric and do not have C_2 symmetry. Each 5′GMP has two possible orientations with H8 above or below the coordination plane. For each LPt(5′GMP)$_2$, four different atropisomers (eight H8 signals) are possible. These four atropisomers may interconvert via sequential rotations. Each ~180° rotation of one 5′GMP about the Pt–N7 bond converts an HT species into an HH species or vice versa. Two ~180° rotations are required to convert one HT into the other HT species or one HH into the other HH species. This relationship is shown schematically for the (*S*,*R*,*R*,*R*)-LPt(5′GMP)$_2$ complex in Figure 2. An important

(25) For a review containing relevant Pt X-ray structures see: Lippert, B. *Prog. Inorg. Chem.* **1989**, *37*, 1.
(26) Reily, M. D.; Marzilli, L. G. *J. Am. Chem. Soc.* **1986**, *108*, 6785.
(27) For other metals see: Miller, S. K.; van der Veer, D. G.; Marzilli, L. G. *J. Am. Chem. Soc.* **1985**, *107*, 1048.
(28) Lippert, B.; Raudaschl-Sieber, G.; Lock, C. J. L.; Pilon, P. *Inorg. Chim. Acta* **1984**, *93*, 43.
(29) Schöllhorn, H.; Raudaschl-Sieber, G.; Müller, G.; Thewalt, U.; Lippert, B. *J. Am. Chem. Soc.* **1985**, *107*, 5932.
(30) Marzilli, L. G.; Iwamoto, M.; Alessio, E.; Hansen, L.; Calligaris, M. *J. Am. Chem. Soc.* **1994**, *116*, 815.
(31) Cramer, R. E.; Dahlstrom, P. L. *J. Am. Chem. Soc.* **1979**, *101*, 3679.
(32) Cramer, R. E.; Dahlstrom, P. L. *Inorg. Chem.* **1985**, *24*, 3420.
(33) Dijt, F. J.; Canters, G. W.; den Hartog, J. H. J.; Marcelis, A. T. M.; Reedijk, J. *J. Am. Chem. Soc.* **1984**, *106*, 3644.
(34) Marcelis, A. T. M.; van Kralingen, C. G.; Reedijk, J. *J. Inorg. Biochem.* **1980**, *13*, 213.
(35) Marcelis, A. T. M.; Korte, H.-J.; Krebs, B.; Reedijk, J. *Inorg. Chem.* **1982**, *21*, 4059.
(36) Marcelis, A. T. M.; van der Veer, J. L.; Zwetsloot, J. C. M.; Reedijk, J. *Inorg. Chim. Acta* **1983**, *78*, 195.
(37) Miller, S. K.; Marzilli, L. G. *Inorg. Chem.* **1985**, *24*, 2421.
(38) Cramer, R. E.; Dahlstrom, P. L.; Seu, M. J. T.; Norton, T.; Kashiwagi, M. *Inorg. Chem.* **1980**, *19*, 148.
(39) Reily, M. D.; Wilkowski, K.; Shinozuka, K.; Marzilli, L. G. *Inorg. Chem.* **1985**, *24*, 37.
(40) Bau, R.; Gellert, R. W. *Biochimie* **1978**, *60*, 1040.

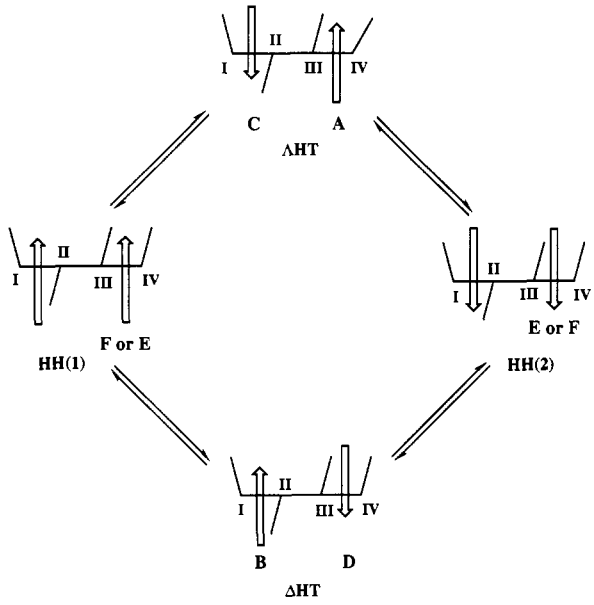

Figure 2. Shorthand representation of the *N,N'*-dimethyl-2,3-diaminobutane platinum(II) complex viewed with the 5'GMP coordination sites forward and the *N,N'*-dimethyl-2,3-diaminobutane ligand to the rear. Roman numerals indicate the labeling system for the chelate ring nitrogens and carbons. The arrows represent 5'GMP molecules, with the head of the arrow denoting H8. Interconversion between head-to-tail and head-to-head atropisomers of (*S,R,R,R*)-LPt(5'GMP)$_2$ is illustrated, as are assignments of signals A–F (see text).

difference between the complexes in this study and those in our earlier study[8] involves the positioning of the NH groups. In the C_2 symmetrical complexes studied earlier both NHs were quasi-axial and on opposite sides of the platinum coordination plane. In the less symmetrical complexes studied here, one NH is quasi-axial but the other is quasi-equatorial and both are on the same side of the platinum coordination plane.

Experimental Section

Materials. 5'GMP (Aldrich) was used as received. The *N,N'*-dimethyl-2,3-diaminobutane ligands were prepared by reduction of dimethylglyoxime with Raney nickel, followed by fractional crystallization of the HCl salts to separate the meso and racemic forms.[41] The racemic mixture was resolved with tartaric acid.[42] The diaminobutane isomer was converted to the bis(trifluoromethyl)amide derivative and dimethylated with methyl iodide in KOH/dimethyl sulfoxide. The trifluoroacetyl groups were removed by HCl in methanol to yield L·2HCl.

LPtCl$_2$ complexes were prepared by substitution of L for (DMSO)$_2$ in *cis*-Pt(DMSO)$_2$Cl$_2$. In a typical experiment a suspension of *cis*-Pt(DMSO)$_2$Cl$_2$ in methanol (0.42 g, 1 mmol, in 90 mL) was treated with a solution containing a stoichiometric amount of L (either the *SS* or the *RR* isomer) in the same solvent (1 mmol in 10 mL). After it was stirred for few hours, the suspension turned to a colorless solution which was then concentrated to a small volume and kept at 5 °C for 1 day. After filtration (to separate a small amount of unchanged *cis*-Pt(DMSO)$_2$Cl$_2$) the solution was dried, and then the solid residue was redissolved in water (30 mL), treated with an excess of LiCl (0.35 g), and kept on a steam bath for 5 h. The yellow precipitate which formed was collected, washed with water, and dried in vacuo; the yield was ≥80%. The compound proved to be a mixture of two LPtCl$_2$ isomers differing in the configuration of the asymmetric nitrogens ((*S,R,R,S*)-LPtCl$_2$ and (*S,R,R,R*)-LPtCl$_2$; (*R,S,S,R*)-LPtCl$_2$ and (*S,S,S,R*)-LPtCl$_2$). The separation of the isomers was accomplished by fractional crystallization. In a typical experiment the product obtained from the above reaction was suspended in a small volume of DMF (10 mL). The suspension was stirred on a steam bath for 10 min and the solution filtered. This procedure was repeated a few times until the DMF remained colorless. The solid residue, which was washed with water and methanol and then dried in vacuo, proved to be the pure symmetrical isomer ((*S,R,R,S*)-LPtCl$_2$ or (*R,S,S,R*)-LPtCl$_2$). The DMF solution, containing the second isomer, was treated with an excess of diethyl ether. The yellow precipitate formed, was collected and recrystallized from DMF/diethyl ether. It proved to be the pure asymmetrical isomer ((*S,R,R,R*)-LPtCl$_2$ or (*S,S,S,R*)-LPtCl$_2$). Anal. Calcd for $C_6H_{16}N_2Cl_2Pt$: C, 18.8; H, 4.2; Cl, 18.5; N, 7.3. Found for (*S,R,R,S*)-LPtCl$_2$: C, 18.8; H, 4.2; Cl, 18.4; N, 7.3. Found for (*S,R,R,R*)-LPtCl$_2$: C, 19.0; H, 4.2; Cl, 18.5; N, 7.3. Found for (*R,S,S,R*)-LPtCl$_2$: C, 18.9; H, 4.3; Cl, 18.6; N, 7.3. Found for (*S,S,S,R*)-LPtCl$_2$: C, 19.1; H, 4.3; Cl, 18.5; N, 7.4.

LPt(SO$_4$) complexes were prepared from the corresponding dichloro complexes by reaction with silver sulfate. In a typical experiment LPtCl$_2$ (1 mmol) was suspended in water (10 mL) and treated with a stoichiometric amount of Ag_2SO_4 (1 mmol). The mixture was kept stirring for 1 day in the dark. The solution was filtered, the solvent evaporated, and the solid residue triturated with diethyl ether, separated from the solution, and dried in vacuo. The yield was ≥90%. Anal. Calcd for $C_6H_{16}N_2O_4SPt$: C, 17.7; H, 3.9; N, 6.8. Found for (*S,R,R,S*)-LPt(SO$_4$): C, 17.3; H, 4.4; N, 6.3. Found for (*S,R,R,R*)-LPt(SO$_4$): C, 17.7; H, 4.4; N, 6.4. Found for (*R,S,S,R*)-LPt(SO$_4$): C, 17.3; H, 4.4; N, 6.3. Found for (*S,S,S,R*)-LPt(SO$_4$): C, 17.7; H, 4.4; N, 6.4.

Methods. Two equivalents of 5'GMP was treated with 1 equiv, ~5 mM, of LPt(SO$_4$) in 0.55 mL D_2O. The small addition of deuterated nitric acid kept the pH (uncorrected) below 4. Maintenance of this pH was essential to prevent hydroxide ion catalyzed isomerization of the asymmetric N centers of the LPt(SO$_4$) and product complexes. The samples were lyophilized and then redissolved in 0.50 mL of 99.96% D_2O.

^{1}H NMR 1D spectra were obtained on a Nicolet NT-360 spectrometer operating at 361.08 MHz and equipped with a variable temperature unit. The 1D NOE spectra were recorded using the residual HOD peak as a reference. A 15-μs pulse was the 90° tip angle. The NOE experiment was performed using a 16K block size and an initial 6-μs pulse followed by a 250-ms delay. The NOE pulse was then applied to the peak of interest for 800 ms at a power of 34 dB. After 128 scans were collected, the FIDs were processed using an exponential multiplication apodization function (em) with a line broadening of 3 Hz.

The 2D data were obtained at 5 °C with a GE/GN 500 MHz spectrometer operating at 500.1 MHz with a spectral window in both dimensions of 4405.29 Hz. Spectra were processed with the FTNMR (Hare, Inc.) or the FELIX program (Hare, Inc.) on a VAX or a Personal IRIS computer, respectively.

The 2D phase-sensitive chemical exchange correlation spectra, NOESY/EXSY, resulted from a 2 × 512 × 2048 matrix with mixing times of 300 and 500 ms, with 32 acquisitions per t_1 period. An em function with a line broadening of 2 Hz was applied in the acquisition dimension and the base line was corrected using a polynomial function of zero order. The evolution dimension was zero filled to 2048 points and a 90° shifted sine bell squared function was applied. To emphasize the first few data points, the FIDs were also processed using an em function with a line broadening of 8 Hz in D1 and a 90° shifted skewed sine bell squared function in D2. Some spectra were symmetrized to eliminate residual noise.

The hypercomplex 2D rotating frame Overhauser enhancement spectra, 2D ROESY, resulted from a 2 × 512 × 2048 matrix with a mixing time of 250 ms, with 16 acquisitions per t_1 period. Spectra were processed as above.

The 2D correlation spectroscopy spectra, COSY, resulted from the collection of 1024 × 2048 matrix, with 16 acquisitions per t_1 period. Spectra were processed in the magnitude mode using an em function and a 90° shifted sine bell function in the evolution and acquisition dimensions, respectively.

Results

(*S,R,R,R*)-LPt(5'GMP)$_2$. In the ^{1}H NMR spectrum for this complex, the 5'GMP H8 signals are in the 7.9–9.0 ppm region at pH 3.5. The downfield shift of the H8 signals compared to those for free 5'GMP[1,26] and the acidic pH used for sample preparation indicate that 5'GMP coordination is via N7. The H8 region has many peaks, but four peaks comprise 82 ± 8% of the H8 intensity (Figure 3). These peaks, at 8.32, 8.40, 8.51, and 8.57 ppm, are designated as A, B, C, and D, respectively. The 1.0–3.5 ppm region contains the NCH$_3$, CCH$_3$, and CH signals of L. The 5.7–6.6 ppm region contains NH signals at 5.79, 6.22,

(41) Dickey, F. H.; Fickett, W.; Lucas, H. J. *J. Am. Chem. Soc.* **1952**, *74*, 944.

(42) Krumholz, P. *J. Am. Chem. Soc.* **1953**, *75*, 2163.

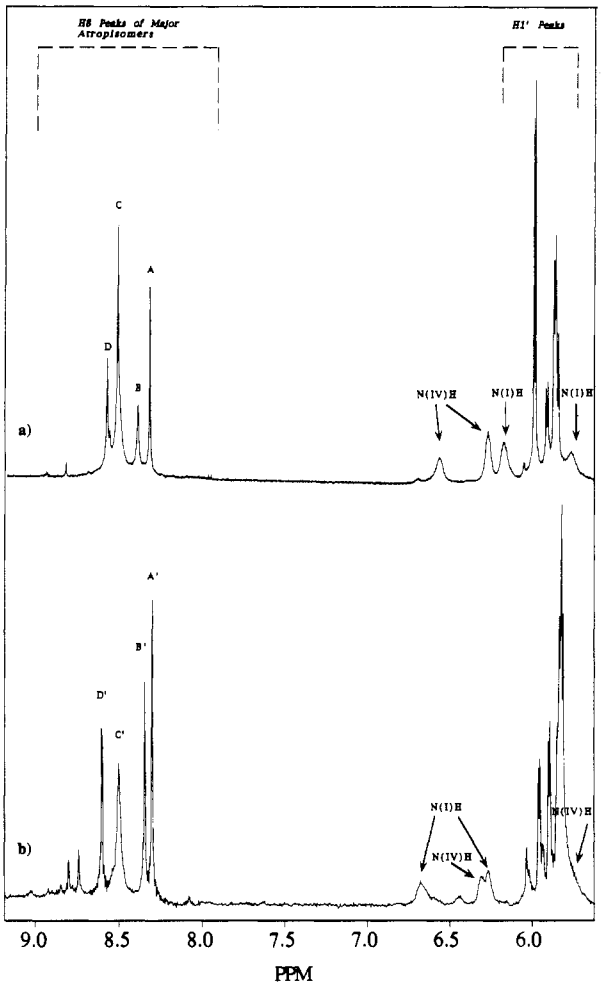

Figure 3. H8 and NH/H1′ region of the 1D spectrum of (a) (*S,R,R,R*)-LPt(5′GMP)$_2$ and (b) (*S,S,S,R*)-LPt(5′GMP)$_2$.

6.29, and 6.58 ppm; these have cross-peaks to the CCH_3, NCH_3, and CH region.

Integration of the H8 region showed that the areas of A and C are equivalent and the areas of B and D are equivalent. On the basis of the sum of the areas (A and C ~46 ± 4%; B and D ~36 ± 4%), A and C are the H8 signals from the major atropisomer and B and D are the H8 signals from the next most abundant atropisomer. An upfield shoulder at 8.55 ppm (~3% of the H8 area) was subtracted from the area of D (Table 1).

1D NOE, NOESY/EXSY (Figure 4), and ROESY experiments showed a connectivity between A and D (i.e. cross-peak A–D) as well as one between B and C, (i.e. cross-peak B–C). In the ROESY spectrum, these cross-peaks are negative, indicating they are due to exchange. These connectivities demonstrate that the 5′GMPs with H8s A and D are bound to the same coordination position (***cp1*** or ***cp2***) and the 5′GMPs with H8s B and C are bound to the other (***cp2*** or ***cp1***).

In the 2D NOESY spectrum, minor H8 signals are found at low contours. Experiments in which either the ratio of 5′GMP to (*S,R,R,R*)-LPt was varied or the appearance of bis product was monitored indicate that four small H8 signals (Table 1) are from the four mono species of the type [(*S,R,R,R*)-LPt(5′GMP)-(H_2O)]$^+$. Other minor H8 signals have been assigned to LPt-(5′GMP)$_2$, where L is a different isomeric form of the ligand (Table 1 and ref 43).

Minor H8 peaks, 8.81 (E) and 8.00 (F) ppm, have cross peaks to both A and D in the NOESY/EXSY spectrum (Figure 4). The area of E is ~2% of the H8 region. Since peak F is broad, its total area is uncertain. The volume of the cross-peak D–E is greater than that for A–E; likewise, the volume of the cross-peak D–F is greater than that for A–F. In the ROESY spectrum, these cross-peaks are negative, indicating that they are caused by chemical exchange. These findings are considered further below, but the connectivity pattern demonstrates that there are two minor (*S,R,R,R*)-LPt(5′GMP)$_2$ atropisomers, in addition to the two major ones.

The H8 signals have NOE cross peaks to NH and NCH_3 signals (Figures 5 and 6). For the major species, a qualitative method was used as a guide for determining the orientation of the H8 of each 5′GMP. This method utilized the distance dependence of NOEs and involved first dividing the volume of the H8–NCH_3 cross-peak by three (to normalize it to one proton) and then dividing the result by the volume of the H8-NH cross-peak. If

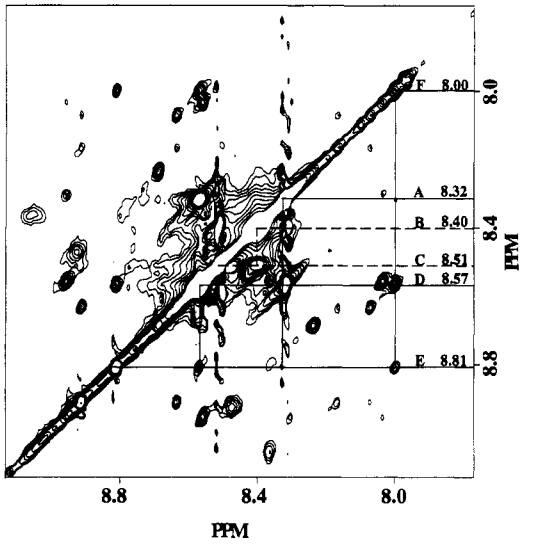

Figure 4. H8 region of the (*S,R,R,R*)-LPt(5′GMP)$_2$ 2D NOESY/EXSY spectrum at a low cut to show the connectivity between the H8s of all the atropisomers in the system, labeled as in the text.

Table 1. Shifts (ppm), Labels, H8 Cross-Peaks (ppm), and Species Assignment for All 5′GMP H8 Signals in the NOESY/EXSY Spectrum of the (*S,R,R,R*)-LPt(5′GMP)$_2$ Sample[a]

H8	label	H8 cross-peaks	assignment
8.32	A	8.57, 8.00, 8.81	(*S,R,R,R*)-LPt(5′GMP)$_2$ ΔHT (***cp2***)
8.40	B	8.51	(*S,R,R,R*)-LPt(5′GMP)$_2$ ΔHT (***cp1***)
8.51	C	8.40	(*S,R,R,R*)-LPt(5′GMP)$_2$ ΔHT (***cp1***)
8.57	D	8.32, 8.00, 8.81	(*S,R,R,R*)-LPt(5′GMP)$_2$ ΔHT (***cp2***)
8.81	E	8.00, 8.32, 8.57	(*S,R,R,R*)-LPt(5′GMP)$_2$ HH (***cp2***)
8.00	F	8.81, 8.32, 8.57	(*S,R,R,R*)-LPt(5′GMP)$_2$ HH (***cp2***)
8.03		8.30, 8.55, 8.96	(*S,R,R,S*)-LPt(5′GMP)$_2$ HH
8.96		8.03, 8.30, 8.55	(*S,R,R,S*)-LPt(5′GMP)$_2$ HH
8.30		8.03, 8.55, 8.96	(*S,R,R,S*)-LPt(5′GMP)$_2$ ΔHT minor
8.55		8.03, 8.30, 8.96	(*S,R,R,S*)-LPt(5′GMP)$_2$ ΔHT major
8.07		8.17, 8.63, 8.91	(*R,S,S,R*)-LPt(5′GMP)$_2$ HH
8.91		8.07, 8.17, 8.63	(*R,S,S,R*)-LPt(5′GMP)$_2$ HH
8.63		8.07, 8.17, 8.91	(*R,S,S,R*)-LPt(5′GMP)$_2$ ΔHT major
8.17		8.07, 8.63, 8.91	(*R,S,S,R*)-LPt(5′GMP)$_2$ ΔHT minor
8.24		8.69	mono adduct
8.69		8.24	mono adduct
8.47		8.92	mono adduct
8.92		8.47	mono adduct

[a] pH 3.5, 5 °C.

(43) Examination of the 2-D NOESY/EXSY spectrum reveals that the upfield shoulder on D, at 8.55 ppm, has cross-peaks to minor H8 signals (each less than 1% of H8 area) (Figure 4). Comparison with the (*S,R,R,S*)-L system shows that several H8 signals are assignable to atropisomers of this isomeric system as follows: 8.55 ppm, ΔHT; 8.03 and 8.96 ppm, HH; 8.30 ppm, ΔHT. Since the (*S,R,R,S*)-L complex has two equivalent coordination sites, i.e. C_2 symmetry, only one HH conformation is possible. Thus, ~7% of the H8 region includes peaks corresponding to the atropisomers of the (*S,R,R,S*)-L system. Evidently, some isomerization of the (*S,R,R,R*)-L conformers has led to the more stable (*S,R,R,S*)-L conformers. A small peak at 8.63 ppm, with ~1–2% of the H8 region, has three cross peaks. Comparison with the (*R,S,S,R*)-L system[8] shows that this small peak is the H8 signal of the ΔHT atropisomer. The cross-peaks to 8.91 and 8.07 ppm are to the HH atropisomer, and that at 8.17 ppm corresponds to the ΔHT atropisomer.

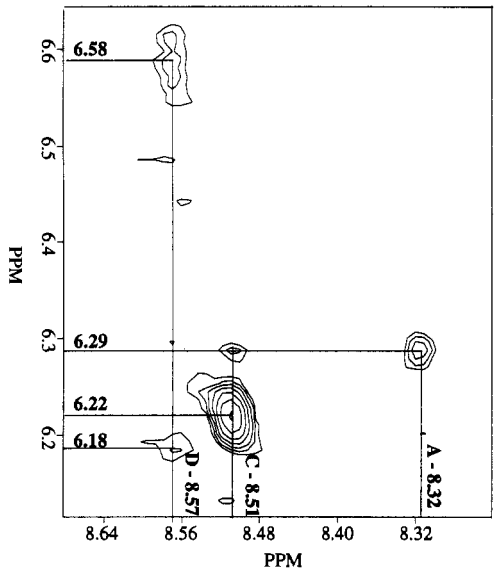

Figure 5. H8–NH cross-peaks of the (*S*,*R*,*R*,*R*)-LPt(5'GMP)$_2$ NOESY spectrum with chemical shifts labeled. The cross-peak at 6.18 ppm is the H8-H1' of ΔHT (*S*,*R*,*R*,*S*)-LPt(5'GMP)$_2$.

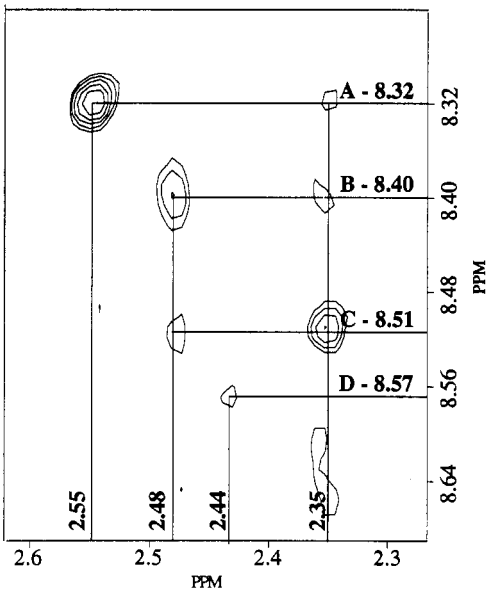

Figure 6. H8–NCH$_3$ cross-peaks of the (*S*,*R*,*R*,*R*)-LPt(5'GMP)$_2$ NOESY spectrum with chemical shifts labeled.

this ratio is greater than one, the group nearest the H8 is an NCH$_3$, but if this ratio is less than one, the group nearest the H8 is an NH. This ratio (Table 2) is greater than one of H8 signals A and B, but less than one for C and D. The H8s with signals A and B are nearest the NCH$_3$s with signals at 2.55 ppm and at 2.48 ppm, respectively. The H8s with signals C and D are nearest the NHs with the signals at 6.22 and 6.58 ppm, respectively. Since the 5'GMPs with H8 signals A and D have the same coordination position (*vide supra*), these must have opposite orientations. This relationship also holds for the 5'GMPs with H8 signals B and C. This method reveals that the significant atropisomers both have the HT conformation, but since there are two possible nonequivalent coordination positions, the method does not distinguish between ΔHT and ΛHT.

The coordination positions of the 5'GMPs can be determined from the known absolute configuration of L[42] in the following manner: From COSY and NOESY/EXSY spectra, the L CH, CCH$_3$, NH, and NCH$_3$ signals were assigned. Since the relative positions of the H8s with respect to NCH$_3$ and NH groups were determined above, assignment of the coordination positions of each 5'GMP was then straightforward.

Table 2. Assignment and Chemical Shifts (ppm) of the NH and NCH$_3$ Signals of the Major Atropisomers of (*S*,*R*,*R*,*R*)-LPt(5'GMP)$_2$ (Also Included H8 to NH and H8 to NCH$_3$ Cross-Peaks, Their Relative Volumes, and One-Third the H8-NCH$_3$/H8-NH Volume Ratio from the 2D NOESY/EXSY Spectrum)

H8	NH (site)	NCH$_3$ (site)	relative vol	(NCH$_3$)/(NH × 3)	comment
A	6.29 (IV)		1.4		
A		2.55 (IV)	10.3	2.4	
A		2.35 (I)	2.8		spin diff[a]
B[b]	5.79 (I)				
B		2.48 (I)	5.1	large	
B		2.35 (I)	2.8		from N(I)CH$_3$ of ΔHT[c]
C	6.22 (I)		5.5	5.5	
C		2.35 (I)	5.9	0.3	
C	6.29 (IV)		0.5		spin diff[a]
C		2.48 (I)	3.2		from N(I)CH$_3$ of ΔHT[c]
D	6.58 (IV)		1.5		
D		2.44 (IV)	2.6	0.6	

[a] 300 and 500 ms mixing times result in spin diffusion from the NH and/or NCH$_3$ through the atoms of L. [b] H8 signal B did not have a visible NH cross-peak. [c] These cross-peaks are due to exchange between the ΛHT and ΔHT atropisomers.

Table 3. Chemical Shifts (ppm), Assignments, Cross-Peak Volumes of L Signals, and H8 Signal from the Nearest 5'GMP for the Major Atropisomers of (*S*,*R*,*R*,*R*)-LPt(5'GMP)$_2$

NH (site)	NCH$_3$ (site)[a]	CH (site)	CCH$_3$ (site)	rel vol	nearest H8
6.29 (IV)			1.19 (III)	5.9	A
6.29 (IV)		3.38 (III)		43.2	A
6.29 (IV)		3.06 (II)		2.9	A
	2.55 (IV)		1.19 (III)	23.2	A
	2.55 (IV)	3.06 (II)		28.3	A
5.79 (I)[b]					B
	2.48 (I)		1.27 (II)	19.8	B
	2.48 (I)	3.07 (II)		19.7	B
6.22 (I)			1.27 (II)	17.0	C
6.22 (I)		3.38 (III)		17.0	C
6.22 (I)		3.06 (II)		6.0	C
	2.35 (I)		1.27 (II)	26.5	C
	2.35 (I)	3.06 (II)		25.9	C
6.58 (IV)			1.19 (III)	0.7	D
6.58 (IV)		3.38 (III)		7.8	D
	2.44 (IV)		1.19 (III)	13.1	D
	2.44 (IV)	3.07 (II)		9.1	D

[a] Only one NCH$_3$–CH or NCH$_3$–CCH$_3$ cross-peak was present; cross-peaks were not observed to the groups farther away, e.g. N(IV)CH$_3$ to C(II)CH$_3$. [b] No visible N(I)H–CH cross-peak was found.

There are three L CH signals (Table 3). The NOESY/EXSY and COSY spectra allow assignment of these CH signals. The CH signal at 3.38 ppm has no NCH$_3$ NOE cross-peak (Figure 7). Of the two CH protons, the C(III)H proton should be farthest from an NCH$_3$ group (Figure 1); therefore this signal is from C(III)H (Table 3). The other two CH signals, 3.06 and 3.07 ppm, each have NOE cross-peaks to two NCH$_3$ signals (Figure 7) and therefore must be from C(II)H. In the COSY spectrum (not shown), the CCH$_3$ signals can be assigned from the CH–CH$_3$ cross-peaks. The downfield C(III)H signal (at 3.38 ppm) has a cross peak to the upfield CCH$_3$ signal (at 1.19 ppm), designating it as C(III)CH$_3$. The C(II)H signals at 3.06 and 3.07 ppm have cross-peaks to the CCH$_3$ signal at 1.27 ppm, indicating that this is the C(II)CH$_3$ signal.

The NOESY/EXSY spectrum was then used to assign the NH and NCH$_3$ signals. The NH signal at 6.29 ppm has cross-peaks to the C(III)H (Figure 8) and C(III)CH$_3$ signals. The NH signal at 6.58 ppm has only one CH cross-peak (to C(III)H, Figure 8). This pattern demonstrates that these NH signals are from N(IV)Hs.

The NH signal at 6.22 ppm has two CH cross-peaks (Table III). The cross-peak to C(II)H has less than half the relative

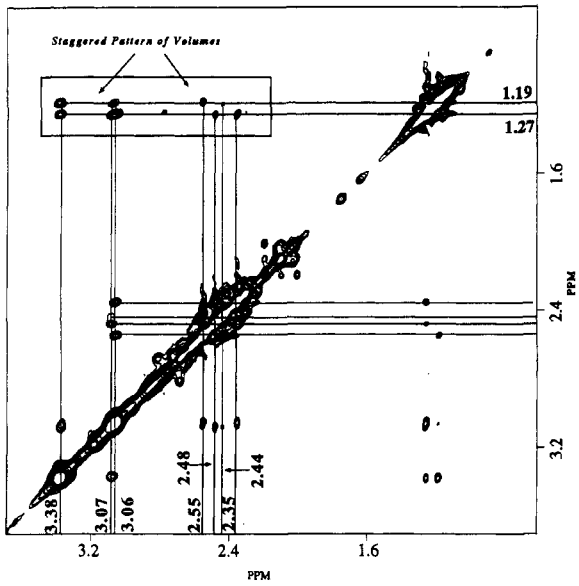

Figure 7. Upfield region of the (*S*,*R*,*R*,*R*)-LPt(5′GMP)$_2$ 2D NOESY/EXSY spectrum. The chemical shifts of the NCH_3, CCH_3, and CH signals are labeled. Arrows indicate the staggered pattern of cross peak volumes.

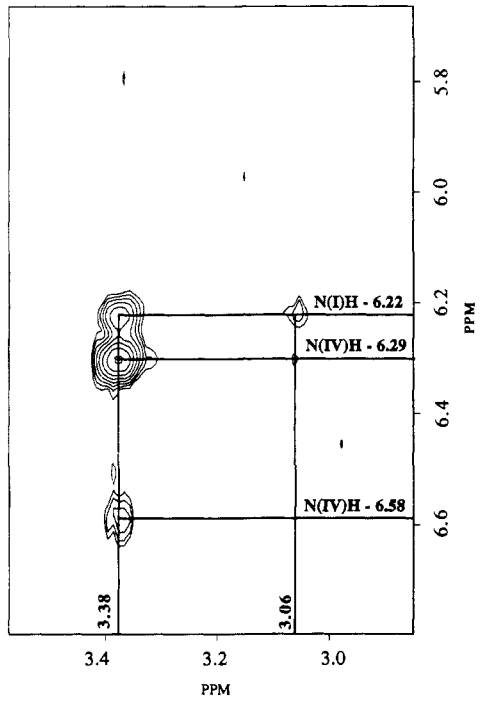

Figure 8. NH–CH cross peaks of the (*S*,*R*,*R*,*R*)-LPt(5′GMP)$_2$ NOESY spectrum with chemical shifts labeled.

volume of the cross-peak to C(III)H (Figure 8). Examination of models suggests that the distance between the C(III)H and N(I)H protons is less than that between C(II)H and N(I)H because the C(III)H and N(I)H protons are on the same side of the N(I)–Pt–N(IV) plane. The NH signal at 6.22 ppm also has a cross-peak to the C(II)CH_3 signal at 1.27 ppm. Therefore, this signal is for N(I)H. The other N(I)H has a signal at 5.79 ppm; see below.

Further support of these assignments and coordination positions comes from patterns of cross-peaks involving the four NCH_3 signals (Table 3). Each of the NCH_3 signals has only one CCH_3 cross-peak (Figure 7). The NCH_3 signals at 2.55 and 2.35 ppm are greater in area than those at 2.48 and 2.44 ppm. Therefore, the former signals are associated with the major atropisomer. The NCH_3 signals at 2.55 and 2.44 ppm each have large cross-peaks to C(III)CH_3 and therefore are assigned to N(IV)CH_3. The remaining NCH_3 signals at 2.48 and 2.35 ppm each have large cross-peaks to C(II)CH_3 and therefore are assigned to N(I)-CH_3s.

The CCH_3–CH region contains an unusual pattern of cross-peaks in which a large volume cross-peak alternates with a small volume cross-peak (Table 3, Figure 7). Such a pattern confirms, as expected, that the C(II)–C(III) bond is skewed with respect to the N(I)–Pt–N(IV) plane. C(II) and C(III) are on opposite sides of this plane such that a line drawn from C(II) to C(III) would have a negative slope, and both C–CH_3 groups are in quasi-equatorial positions, i.e., the chelate has the λ conformation. Examination of PtL models in this skewed conformation demonstrates not only that the distance between methyl groups is maximized but also that the distance between protons C(III)H and N(I)H is less than C(II)H and N(I)H. This model is supported by the larger cross-peak between C(III)H and N(I)H compared to that between C(II)H and N(I)H.

Information from the 1D, COSY, NOESY/EXSY, and ROESY spectra can be used to define the chirality of the two predominant atropisomers of the (*S*,*R*,*R*,*R*)-LPt(5′GMP)$_2$ system. The 5′GMPs with H8 signals A and D were shown to be closest to the NCH_3 with a signal at 2.55 ppm and to the NH with a signal at 6.58 ppm, respectively; therefore, they are at ***cp2***. On the other hand, the 5′GMPs with H8 signals B and C were shown to be closest to the NCH_3 with a signal at 2.48 ppm and to the NH with a signal at 6.22 ppm, respectively; therefore, they are at ***cp1***. In the most abundant atropisomer, the 5′GMPs with H8 signals A and C are t ***cp2*** and ***cp1***, respectively. The H8 with signal A is nearest to N(IV)CH_3, and the H8 with signal C is nearest to N(I)H. This major atropisomer thus has the ΛHT conformation (Figure 9). In the next most abundant atropisomer, the 5′GMPs with H8 signals D and B are at ***cp2*** and ***cp1***, respectively. The H8 with signal D (exchanging with the H8 with signal A) is nearest N(IV)H. The H8 with signal B (exchanging with the H8 with signal C) is nearest N(I)CH_3. The minor atropisomer thus has the ΔHT conformation (Figure 9).

Let us now consider the unusual upfield shift (5.79 ppm) of the N(I)H signal of the ΔHT (*S*,*R*,*R*,*R*)-LPt(5′GMP)$_2$ atropisomer. Since this signal had no clear NOE cross-peaks to signals of nonexchangeable protons, we first wished to ensure that the assignment of this shift was correct since all the other NH signals were downfield of 6 ppm. First, careful adjustment of the pH allowed D-exchange of all the NH signals including the unusual upfield N(I)H signal. Second, close examination of a deep cut of the COSY spectrum revealed an N(I)H to N(I)CH_3 cross-peak. Third, a deep cut of the NOESY spectrum revealed an N(I)H to N(I)H EXSY cross-peak between the two HT atropisomers. Since the partner N(I)H signal has a fairly normal shift at 6.22 ppm, this is strong evidence for the correctness of the assignments. Furthermore, there is a similar upfield NH peak assignable to N(IV)H of the ΛHT (*S*,*S*,*S*,*R*)-LPt(5′GMP)$_2$ atropisomer; this assignment is supported by an N(IV)H to N(IV)H EXSY cross-peak.

The pH dependence of the NH shifts is also of interest. Identifying the NH signal by the letter used to identify the H8 signal of the cis 5′GMP, we find that the upfield N(I)H signal at 5.79 ppm did not shift significantly as the pH was raised to above 6 (supplementary material). The N(I)H of the other atropisomer, signal C, shifted downfield. Likewise for N(IV)H, only one (D) shifted significantly while the other (A) shifted very little. Thus, for each atropisomer, only one of the two NH signals shifted significantly.

The H8 region of the NOESY spectrum of the (*S*,*R*,*R*,*R*)-LPt(5′GMP)$_2$ complex has a unique connectivity pattern between A and D H8 signals of the two HT atropisomers and two H8 peaks labeled E and F (Figure 5, Table 1). (A similar connectivity pattern is not seen in (*S*,*S*,*S*,*R*)-LPt(5′GMP)$_2$ spectra.) E and F must represent H8 signals from one or both HH atropisomers

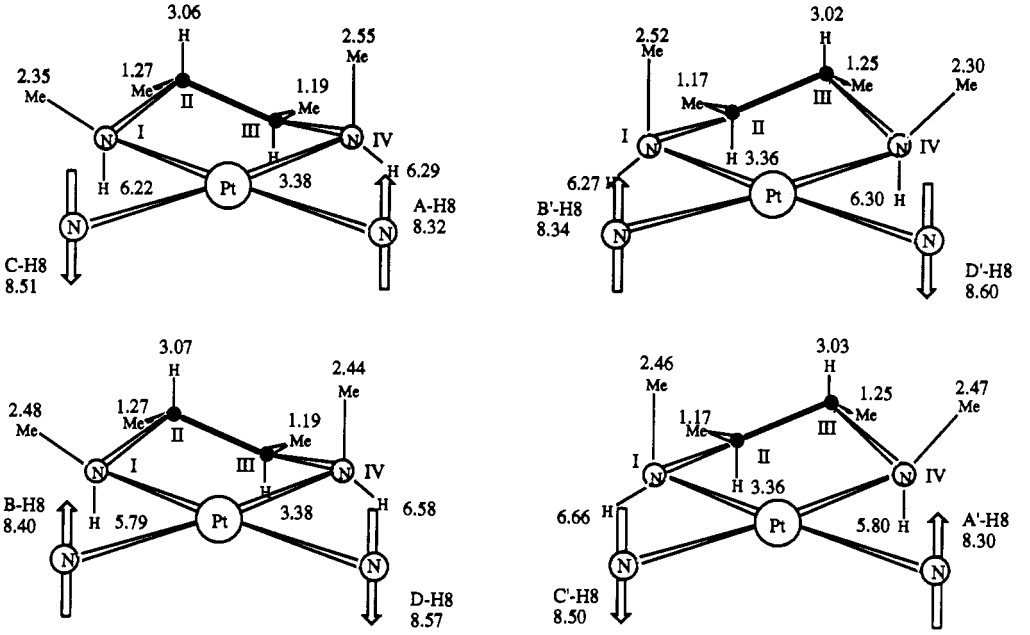

Figure 9. Schematic diagrams of the ΛHT (*top left*) and ΔHT (*bottom left*) atropisomers of (*S,R,R,R*)-LPt(5'GMP)$_2$ and the ΛHT (*top right*) and ΔHT (*bottom right*) atropisomers of (*S,S,S,R*)-LPt(5'GMP)$_2$ viewed with the 5'GMP coordination sites forward and the *N,N'*-dimethyl-2,3-diaminobutane ligand to the rear. The heads of the arrows represent the orientation of the H8 of 5'GMP. The values listed are chemical shifts in ppm, and the chelate rings are in the λ and δ conformations for the (*S,R,R,R*)-LPt(5'GMP)$_2$ and the (*S,S,S,R*)-LPt(5'GMP)$_2$, respectively.

for two reasons. First, only two different HT atropisomers are possible and have been identified. Second, the ~0.8 ppm chemical shift difference between E and F is comparable to the ~1.0 ppm chemical shift difference between the H8s of the HH atropisomer in previous studies involving (*R,S,S,R*)-LPt(5'GMP)$_2$ and (*S,R,R,S*)-LPt(5'GMP)$_2$.[8]

The coordination position of the 5'GMPs with H8 signals E and F can be determined from the pattern of cross-peaks involving these signals in the (*S,R,R,R*)-LPt(5'GMP)$_2$ spectra. The pattern of cross-peaks does not include both 5'GMP coordination positions; the only cross-peaks visible to E and F are from A and D, both for ***cp2***. Thus, E and F are the H8 signals from the 5'GMPs at ***cp2*** in the two HH atropisomers; these 5'GMPs have opposite orientations and are linked via rotation through the HT atropisomers.

(*S,S,S,R*)-LPt(5'GMP)$_2$. This system is similar to the (*S,R,R,R*)-**L** system; therefore the assignment strategy and the determination of coordination position were similar. The (*S,S,S,R*)-**L** system has four major peaks, comprising ~76 ± 8% of the area in the H8 region, as well as many minor peaks (Figure 3). These major peaks, at 8.30, 8.34, 8.50, and 8.60 ppm, are labeled A', B', C', and D', respectively. Integration of the H8 region showed that the areas of A' and C' are equivalent and the areas of B' and D' are equivalent. The sum of the areas of A' and C' is almost equivalent to that of B' and D' (~40 ± 4% vs ~36 ± 4%, respectively). Therefore, there are two major atropisomers, with one only slightly preferred over the other. A downfield shoulder (~7% of the total area) was subtracted from the area of C' (Table 4).

1D NOE experiments and the H8 region of the NOESY/EXSY spectrum showed connectivities between A' and D' and between B' and C' (Figure 10). In the ROESY spectrum, these cross-peaks are negative, indicating exchange. The 5'GMPs with H8 signals A' and D' are bound at the same position (***cp1*** or ***cp2***), whereas the 5'GMPs with H8 signals B' and C' are bound at the other position (***cp2*** or ***cp1***). Other minor H8 signals have been assigned to the four mono species of the type [(*S,S,S,R*)-LPt(5'GMP)(H$_2$O)]$^+$ or to LPt(5'GMP)$_2$, where **L** is a different isomeric form of the ligand (Table 4 and ref 44).

The orientation of the 5'GMP H8 with respect to the platinum coordination plane was determined by the ratio method described above. The ratio is greater than one for H8 signals A' and B' (Table 5), indicating that the group nearest the respective H8s is an NCH_3. Furthermore, the ratio is less than one for H8 signals C' and D' (Table 5), indicating that the group nearest these H8s is an NH. The H8 with signal A' is nearest to the NCH_3 with a signal at 2.47 ppm. This H8 also has a weak cross-peak to the NH with a signal at 5.8 ppm. The H8 with signal B' is nearest to the NCH_3 with a signal at 2.52 ppm. The H8 with signals C' and D' are nearest to the NH groups with the

Table 4. Shifts (ppm), Labels, H8 Cross-Peaks, and Species Assignment for All 5'GMP H8 Signals in the NOESY/EXSY Spectrum of the (*S,S,S,R*)-LPt(5'GMP)$_2$ Sample[a]

H8	label	H8 cross-peaks	assignment
8.30	A'	8.60	(*S,S,S,R*)-LPt(5'GMP)$_2$ ΛHT (***cp2***)
8.34	B'	8.50	(*S,S,S,R*)-LPt(5'GMP)$_2$ ΔHT (***cp1***)
8.50	C'	8.34	(*S,S,S,R*)-LPt(5'GMP)$_2$ ΛHT (***cp1***)
8.60	D'	8.30, 8.89	(*S,S,S,R*)-LPt(5'GMP)$_2$ ΔHT (***cp2***)
8.73		8.07, 8.26, 8.92	(*R,S,S,R*)-LPt(5'GMP)$_2$ ΔHT major
8.92		8.07, 8.26, 8.73	(*R,S,S,R*)-LPt(5'GMP)$_2$ HH
8.07		8.26, 8.73, 8.92	(*R,S,S,R*)-LPt(5'GMP)$_2$ HH
8.26		8.07, 8.73, 8.92	(*R,S,S,R*)-LPt(5'GMP)$_2$ ΔHT minor
8.50		8.00, 8.20, 8.89	(*S,R,R,S*)-LPt(5'GMP)$_2$ ΔHT major
8.00		8.20, 8.50, 8.89	(*S,R,R,S*)-LPt(5'GMP)$_2$ HH
8.89		8.00, 8.20, 8.50	(*S,R,R,S*)-LPt(5'GMP)$_2$ HH
8.84		8.17	mono adduct
8.17		8.84	mono adduct
8.36		9.03	mono adduct
9.03		8.36	mono adduct

[a] pH 3.5; 5 °C.

(44) The 1-D and 2-D spectra also contain a peak at 8.73 ppm constituting ~17% of the total area in the H8 region (Figures 3b and 10). Comparison with spectra for the (*R,S,S,R*)-**L** complex previously assigned shows that the peak at 8.73 ppm corresponds to the H8 signal of the 5'GMP of the major atropisomer with ΛHT conformation. This peak, at 8.73 ppm, has connectivity to peaks at 8.07, 8.92, and 8.26 ppm. The first two correspond with the HH and the last with the ΔHT atropisomers, respectively. Only one HH is possible because (*R,S,S,R*)-**L** has C_2 symmetry. As found for the (*S,R,R,R*)-**L** complex, some (*S,S,S,R*)-**L** form probably has isomerized to the more stable (*R,S,S,R*)-**L** form. The downfield shoulder on C' has three cross peaks to H8 signals, each with ~1% of the H8 area (Table 3). Comparison with previous spectra showed that the C' shoulder was from the major ΔHT (*S,R,R,S*)-LPt(5'GMP)$_2$ species. Two peaks, at 8.89 and 8.00 ppm, are from the (*S,R,R,S*)-LPt(5'GMP)$_2$ HH atropisomer and the third, at 8.20 ppm, is from the minor ΛHT atropisomer.

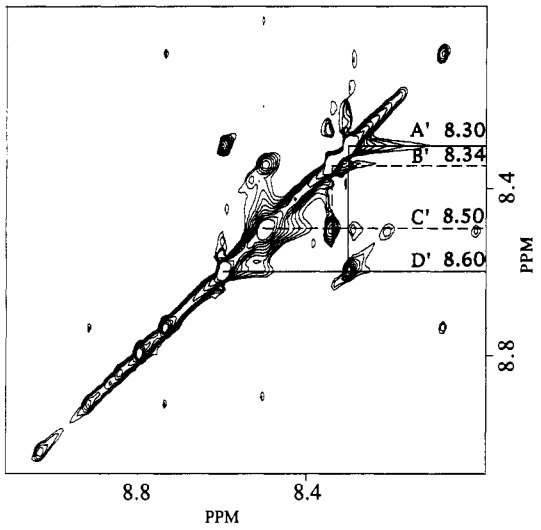

Figure 10. H8 region of the (*S,S,S,R*)-LPt(5'GMP)$_2$ NOESY/EXSY spectrum at a low cut to show the connectivity between the H8s of all the HT atropisomers in the system. The H8s are labeled as in the text.

Table 5. Assignment and Chemical Shifts (ppm) of the NH and NCH_3 Signals of the Major Atropisomers of (*S,S,S,R*)-LPt(5'GMP)$_2$ (Also Included H8 to NH and H8 to NCH_3 Cross-Peaks, Their Relative Volumes, and One-Third the H8-NCH_3/H8-NH Volume Ratio from the 2D NOESY/EXSY Spectrum)[a]

H8	NH (site)	NCH_3 (site)	rel vol	$(NCH_3)/(NH \times 3)$
A'[b]	5.8 (IV)			
A'		2.47 (IV)	13.1	large
B'	6.27 (I)		1.6	
B'		2.52 (I)	10.6	2.2
C'[c]	6.66 (I)		2.4	
C'		2.46 (I)		small
D'	6.30 (IV)		4.5	
D'		2.30 (IV)	4.0	0.3

[a] There are H8–NH cross-peaks at 8.73 and 6.63 ppm due to the (*R,S,S,R*)-LPt(5'GMP)$_2$ ΔHT species. [b] No clear A'–NH cross-peak was visible. [c] The NCH_3 signal had no visible cross-peak to C', but did show cross-peaks to the CH and CCH_3 signals.

signals at 6.66 and 6.30 ppm, respectively (Table 5). Since the 5'GMPs with H8 signals A' and D' have the same coordination position (*vide supra*), these must have opposite orientations. This relationship also holds for the 5'GMPs with H8 signals B' and C'. This information suggests that both atropisomers have the HT conformation, but the coordination position of the 5'GMPs must be determined in order to distinguish between the ΔHT and ΛHT conformations. To accomplish this goal, the CH, CCH_3, NH, and NCH_3 signals were assigned (I, II, III, or IV). Next, the NCH_3 to H8 or NH to H8 cross-peaks were used to determine the coordination position of each 5'GMP.

The 1.0–3.5 ppm region for the (*S,S,S,R*)-L(5'GMP)$_2$ complex contains four large NCH_3 signals, i.e., a pair of signals from each major atropisomer, three CH signals, and two CCH_3 signals. The signals from the CCH_3, NCH_3, and CH regions have cross-peaks to NH signals.

Assignment of the three CH signals is straightforward. The largest CH signal at 3.36 ppm has no NCH_3 cross-peak. Therefore, this signal is from the C(II)H of both major atropisomers. The other two CH signals, at 3.03 and 3.02 ppm, each have cross-peaks to two NCH_3 signals and hence are from C(III)H. The signal at 1.17 ppm is assigned to C(II)CH_3 and the signal at 1.25 ppm is assigned to C(III)CH_3 based on the CH–CH_3 NOE cross peak intensities. The alternating pattern of CH–CH_3 cross-peak volumes (Table 6) confirms as described above that both C–CH_3 groups are in quasi-equatorial positions and that the chelate has the δ conformation. We reiterate that the distance from the C(II)H to the N(IV)H protons is less than that from C(II)H to N(I)H.

Table 6. Chemical Shifts (ppm), Assignments, Cross-Peak Volumes of L Signals and H8 Signal from the Nearest 5'GMP for the Major Atropisomers of (*S,S,S,R*)-LPt(5'GMP)$_2$

NH (site)	NCH_3 (site)	CH (site)	CCH_3 (site)	rel vol	nearest H8
5.8 (IV)[a]					A'
5.8 (IV)		3.36 (II)		1.2	A'
	2.47 (IV)		1.25 (III)	24.3	A'
	2.47 (IV)	3.03 (III)		18.2	A'
6.27 (I)			1.17 (II)	6.4	B'
6.27 (I)		3.36 (II)		27.2[b]	B'
	2.52 (I)		1.17 (II)	25.0	B'
	2.52 (I)	3.02 (III)		5.9	B'
6.66 (I)			1.17 (II)	4.2	C'
6.66 (I)		3.36 (II)		16.8	C'
	2.46 (I)		1.17 (II)	7.1	C'
	2.46 (I)	3.03 (III)		17.5	C'
6.30 (IV)[c]			1.25 (IV)		D'
6.30 (IV)		3.02 (III)		4.6	D'
6.30 (IV)		3.36 (II)		27.2[b]	D'
	2.30 (IV)		1.25 (III)	18.6	D'
	2.30 (IV)	3.02 (II)		17.2	D'

[a] No cross-peak to CCH_3 was visible. [b] Overlapped cross peaks prevented complete resolution; therefore, the reported relative volume is a sum of the large 6.27–3.36 ppm and small 6.30–3.36 ppm cross-peak. [c] T1 noise prevented a volume estimate.

The four NH signals can each be assigned. The NH signal at 6.27 ppm is assigned to N(I)H from the very large cross-peak to the C(II)H signal at 3.36 ppm. Moreover, the NH signals at 6.27 and 6.66 ppm each have a cross-peak to the C(II)CH_3 signal, indicating that both signals arise from N(I)H (Table 6). The NH signal at 6.30 ppm has cross-peaks to C(II)H (large) and to C(III)H (small) signals (Table 6) and must be for an N(IV)H. This N(IV)H signal has a NH–NH cross peak to the 5.8 ppm NH signal which also must be an N(IV)H signal.

The four NCH_3 signals each have one cross-peak to a CCH_3 signal. The NCH_3 signals at 2.47 and 2.30 ppm have cross-peaks to the C(III)CH_3 signal at 1.25 ppm, indicating that they are for N(IV)CH_3. The two other NCH_3 signals, at 2.46 and 2.52 ppm, have cross-peaks to the C(II)CH_3 with signal at 1.17 ppm, indicating that they are from N(I)CH_3.

The N(I)H with the 6.27 ppm signal is nearest to the H8 with signal B', and the N(I)H with the 6.66 ppm signal is nearest to the H8 with signal C'. The N(I)CH_3 signals at 2.46 and 2.52 ppm have cross-peaks to H8 signals at B' and C'. Thus, the 5'GMPs with H8 signals B' and C' are at ***cp1***. The N(IV)H with signal at 6.30 ppm is nearest to the H8 with signals D'. The N(IV)CH_3s with signals at 2.30 and 2.47 ppm are nearest the H8 with signals A' and D'. Thus the 5'GMPs with H8 signals A' and D' are at ***cp2***.

For the 40% HT (*S,S,S,R*)-LPt(5'GMP)$_2$ atropisomer, the H8 at ***cp2*** with signal A' is nearest N(IV)CH_3 and the H8 at ***cp1*** with signal C' is nearest to N(I)H; therefore, this atropisomer has the ΔHT conformation (Figure 9). For the 36% HT atropisomer, the H8 at ***cp2*** with signal D' is exchanging with the H8 with signal A' and is nearest N(IV)H and the H8 at ***cp1*** with signal B' is exchanging with the H8 with signal C' and is nearest N(I)CH_3; therefore, the 36% atropisomer has the ΔHT conformation (Figure 9).

As for the *S,R,R,R* complex, the pH dependence of the NH shifts is also of interest. Identifying the NH signals by the letter used to identify the H8 signal of the cis 5'GMP, we find that the upfield A' N(IV)H signal at 5.8 ppm did not shift significantly as the pH was raised to above 6 (supplementary material). The N(IV)H of the other atropisomer, signal D', shifted downfield. Likewise for N(I)H, only one (C') shifted significantly while the other (B') shifted very little. Thus, as for the *S,R,R,R* HT atropisomers, only one of the NH signals for each *S,S,S,R* HT atropisomer shifted significantly.

Discussion

An important goal of this research was to determine factors which influenced the stability of the atropisomers formed. In particular, we were interested in assessing potential H-bonding interactions, possible steric interactions, and finally any internucleotide interactions. It should be noted that 2D NMR is a powerful method in detecting small amounts of species not readily distinguished from noise in typical 1D NMR experiments. In both systems studied here, the 1D spectra show essentially two dominant atropisomers. Most other species can be detected only along the diagonal in the 2D spectra. Our main focus will be to discuss the more stable species and to assess the factors that influence their stability.

As discussed in the Introduction, four nonequivalent atropisomers are possible in the two systems. We found that for (*S*,*R*,*R*,*R*)-LPt(5′GMP)$_2$ the two predominant atropisomers are HT (~10:1, HT:HH). For (*S*,*S*,*S*,*R*)-LPt(5′GMP)$_2$, the HT:HH ratio is large but cannot be determined because the HH signals were not found. The ΛHT conformation is preferred for both (*S*,*R*,*R*,*R*)-LPt(5′GMP)$_2$ (1.3:1 ΛHT:ΔHT at pH 3.5) and (*S*,*S*,*S*,*R*)-LPt(5′GMP)$_2$ (~1.1:1 ΛHT:ΔHT at pH 3.5).

As presented in Figure 9, the two systems have the *S* NH(CH$_3$) group on the left. However, because of the quasi-equatorial nature of the CCH$_3$ groups, the chelate rings have λ and δ conformations for the (*S*,*R*,*R*,*R*)-LPt and (*S*,*S*,*S*,*R*)-LPt chelate rings, respectively. Thus in Figure 9 the N(I) groups on the left in the (*S*,*R*,*R*,*R*)-LPt system and the N(IV) groups on the right in the (*S*,*S*,*S*,*R*)-LPt system have an equatorial methyl and a quasi-axial NH group. The complementary relationship holds for the other groups. The chemical shifts of the relevant halves of the different systems are closely related. For example, the relationship of the guanine base in the N(I) half of the ΛHT form of (*S*,*R*,*R*,*R*)-LPt(5′GMP)$_2$ is similar to that in the N(IV) half of the ΔHT form of (*S*,*S*,*S*,*R*)-LPt(5′GMP)$_2$. This similarity suggests similar interactions, geometries, etc. and adds confidence to our shift assignments and to our conclusion about the conformations of the atropisomers.

Note that the asymmetry of the sugar breaks the enantiomeric relationship between the *S*,*R*,*R*,*R* and *S*,*S*,*S*,*R* species in the same row of Figure 9 [i.e., between ΛHT (*S*,*R*,*R*,*R*)-LPt(5′GMP)$_2$ and ΔHT (*S*,*S*,*S*,*R*)-LPt(5′GMP)$_2$ (top row) and between ΔHT (*S*,*R*,*R*,*R*)-LPt(5′GMP)$_2$ and ΛHT (*S*,*S*,*S*,*R*)-LPt(5′GMP)$_2$ (bottom row)]. However, the chemical shifts of the "quasi-enantiomeric" pair of complexes are similar, ≤0.08 ppm for **L** and ≤0.10 ppm for 5′GMP H8 signals.

The slight stability of the ΛHT (*S*,*R*,*R*,*R*)-LPt(5′GMP)$_2$ atropisomer over the Δ atropisomer became greater as the pH was raised. The Λ/Δ ratio was 1.3:1 at pH 2.5 (from pH titration data) and increased to ~2.3:1 at pH 6.1. In the case of (*S*,*S*,*S*,*R*)-LPt(5′GMP)$_2$, on the basis of the "quasi-enantiomeric" relationship between atropisomers in the same row of Figure 9, we would have expected the Δ atropisomer to be more stable than the Λ atropisomer. However, this was not the case, and the Λ atropisomer was again more favored. Although the Λ/Δ ratio was only ~1.1:1 at pH 2.5, it increased to ~2:1 at pH ~7. If the guanine ligands had no attached asymmetric groups, a change in preference from the Λ to the Δ HT atropisomer must occur between the *S*,*R*,*R*,*R* and *S*,*S*,*S*,*R* systems. Thus, the small preference for the Λ HT atropisomer for both systems must be induced by the asymmetric sugar–phosphate group which, in the present case, overcomes any preference for either of the two atropisomers induced by the asymmetry of the **L** ligand.

The downfield shift of the NH protons of the diamine in the different atropisomers can give an indication of the occurrence of hydrogen bonding between an NH and the *cis* 5′GMP.[14] Possible H-bonding modes can be assessed from models. The O6 can participate in H-bonding only when the O6 and the NH are on the same side of the coordination plane. When, instead, the H8 and the NH are on the same side, only phosphate group H-bonding is possible. In the normal *anti* conformation of 5′GMP, the phosphate group is close to H8 and, thus, NH. Because the sugar moiety is flexible and there is relatively free rotation about the glycosyl bond, it is possible to form an H-bond between the phosphate group and the NH when the H8 and NH are on opposite sides of the coordination plane.

The NH signals for both ends of the diamine for the atropisomers in the top row of Figure 9 have a moderately downfield shift (6.22–6.30 ppm), suggesting that both NHs are involved in H-bonds of medium strength. In both complexes, one guanine O6 is on the same side as NH with respect to the platinum coordination plane and, in principle, could form an O6–NH H-bond. However, for the same guanine, there is a very intense H8–NCH$_3$ NOE cross-peak, and it could be argued that, with H8 close to NCH$_3$, the O6 end of the guanine is tilted away from the NH. If this is the case, a ROPO$_3$–NH H-bond must be invoked. Because the 5′GMP is less strained in the preferred *anti* conformation, such an H-bond is expected to be less favorable. Indeed, there is no significant downfield NH shift with pH. For the second guanine of the complexes in the top row of Figure 9, an O6–NH H-bond can be excluded since O6 and NH are on opposite sides of the platinum coordination plane. Therefore, if an H-bond is formed, this H-bond must necessarily involve the phosphate group. Indeed, when the pH was raised, the signals for the two quasi-axial NH groups (C and D′, top row of Figure 9) shifted downfield further (supplementary material). Such a downfield shift is consistent with stronger ROPO$_3$–NH H-bonding caused by deprotonation of the phosphate group. The similar pH dependence of the shifts for the quasi-enantiomeric pairs is another piece of evidence confirming the consistency of our assignments for the two complexes.

For the complexes in the bottom row of Figure 9, the downfield shifts suggest that the quasi-equatorial NH (shifts 6.58–6.66 ppm) is involved in a strong hydrogen bond, while the upfield shifts suggest the quasi-axial NH (shifts 5.79–5.80 ppm) is either not involved in H-bonding or is involved in very weak H-bonding. For both complexes, the 5′GMP which is cis to and can interact with the quasi-equatorial NH has O6 on the opposite side of the coordination plane. Therefore, the H-bond must involve the phosphate group; the rather downfield shift suggests a rather strong ROPO$_3$–NH interaction. The quasi-axial NH, which does not appear to be involved in H-bonding, is on the same side as the O6 of the cis 5′GMP. The reason for the failure of an O6–NH H-bond to form most probably lies in the tilting of the guanine base such that O6 is away from the NH. This tilting is caused by interactions with the guanine in the other coordination position; the orientation of this *cis* guanine is dictated by the strong ROPO$_3$–NH H-bond.

Just as for the quasi-enantiomeric pair in the top row of Figure 9, the quasi-enantiomeric pair in the bottom row of Figure 9 has significant pH dependence for only one NH signal per atropisomer (D and C′). These quasi-equatorial NHs can interact with the phosphate group of an anti 5′GMP and this H-bonding should become more favorable when the phosphate group is deprotonated. Thus, the downfield shifts with pH support the occurrence of H-bonding in this case.

The more symmetrical (*S*,*R*,*R*,*R*)-LPt(5′GMP)$_2$ and (*R*,*S*,*S*,*R*)-LPt(5′GMP)$_2$ complexes studied previously, with quasi-axial NHs on opposite sides of the platinum coordination plane, have only three possible atropisomers (two HT and only one HH). One HT atropisomer was greatly favored over the other HT atropisomer, and the stability of the less favored HT atropisomer was comparable to that of the HH atropisomer.[8] The favored HT atropisomer could form two O6–NH H-bonds, the HH atropisomer could form one O6–NH H-bond and the other HT

atropisomer could not form any O6–NH H-bond. Thus, O6–NH H-bonds appeared to dominate the stereochemistry of the complexes.

If one type of H-bonding in isolation determined the atropisomer formed for the (*S*,*R*,*R*,*R*)-LPt(5′GMP)$_2$ and (*S*,*S*,*S*,*R*)-LPt-(5′GMP)$_2$ compounds, one HH form would dominate. If O6–NH H-bonding was most influential, we would have seen predominantly HH(1), Figure 2. If phosphate H-bonding dominated, we would expect primarily HH(2). This investigation has shown that the HT atropisomers are preferred over the HH atropisomers. There appears to be no significant preference for either O6–NH or ROPO$_3$–NH H-bonds. Another feature of our results that suggest that one type of H-bonding is not dominant is the finding that although the ΛHT atropisomer is preferred in both the *S*,*R*,*R*,*R* and *S*,*S*,*S*,*R* systems, this atropisomer is in different rows in Figure 9, meaning that the H-bonding is different. Furthermore, in both cases, raising the pH favored the ΛHT atropisomer.

If indeed there is no significant preference for either O6–NH or ROPO$_3$–NH H-bonds, one might expect the two HT and the two HH atropisomers to be present in comparable amounts. However, the two HT atropisomers dominate. Therefore, the preference for the HT atropisomers must stem from factors other than H-bonding. One factor could be an internucleotide interaction (a type of molecular recognition). It should be noted that in the case of LPt(guanosine)$_2$ complexes with L = tertiary diamine,[31] for which H-bonding cannot be an important factor, the prevailing atropisomers always have the HT conformation. Furthermore, in most cases where the evidence is clear, either in solution or solid states, the HT forms dominate. Additionally, although the ΔHT atropisomer has been found almost exclusively in solid M(5′GMP)$_2$ complexes, in solution the Λ- and ΔHT atropisomers generally have been shown to have comparable stabilities. Thus, the crystallization process may favor the ΔHT atropisomer. The (*S*,*R*,*R*,*R*)-LPt(5′GMP)$_2$ and (*R*,*S*,*S*,*R*)LPt-(5′GMP)$_2$ complexes appear to be a very special case with only one HT atropisomer dominating and with the HH species having significant stability. Thus, O6–NH (axial) H-bonds may be of somewhat greater stability than ROPO$_3$–NH (axial) H-bonds; in conjunction with the preference for HT species, these H-bonds may tip the balance slightly in favor of the species observed.

Acknowledgment. We thank the NIH (Grant GM 29222) and MURST and EC (Contract C11-CT92-0016) for support.

Supplementary Material Available: Figures showing selected regions of NOESY spectra (H8–H1′ of (*S*,*R*,*R*,*R*)-LPt(5′GMP)$_2$; H8–NH, H8–NCH$_3$, NH–CH, and upfield region of (*S*,*S*,*S*,*R*)-LPt(5′GMP)$_2$), plots of the pH dependency of the NH signals from (*S*,*R*,*R*,*R*)-LPt(5′GMP)$_2$ and (*S*,*S*,*S*,*R*)-LPt(5′GMP)$_2$, and tables of H8–H1′ cross-peaks for the two complexes (9 pages). Ordering information is found on any current masthead page.